Forced Response of Plate with Viscoelastic Auxetic Dampers

Tomasz STREK
Poznan University of Technology, Institute of Applied Mechanics
ul. Jana Pawła II 24, 60-965 Poznan
tomasz.strek@put.poznan.pl

Abstract

The example studies a forced response of plate with viscoelastic auxetic damper located at the free end of the plate. Damping elements consist of the cover layer and layer of viscoelastic material with positive or negative Poisson's ratio. Viscoelastic materials are often used for reduction of vibration (seismic or wind induced vibrations in building structures or other structures). The common feature is that the frequency of the forced vibrations is low. Calculations are made using finite element method with Comsol Multiphysics software.

Keywords: auxetic, viscoelastic, damper, finite element method

1. Introduction

One of the first mentions of materials with negative Poisson's ratio (NPR) can be found in 1981 and 1982 [1-4]. Theoretical and experimental values of PR for rubber models showed that PR value can be negative [1]. Lora Jane Gibson [1] analyzed a model of cellular material as a simple, two-dimensional array of hexagonal cells and identify and analyze the mechanisms by which it deforms. From this Gibson calculated the elastic moduli and the elastic and plastic collapse stresses for ideal two-dimensional cellular materials. Experimentally verified results showed that mechanical properties depend on three parameters: a solid cell wall material property, a geometric constant, and the relative density of the cellular material raised to the power two or three. A few years later Almgren [5] and Wojciechowski [6] showed respectively mechanical and thermodynamical model of materials with auxetic behavior.

In 1987 Lakes developed foams with negative Poisson’s ratio [7-8]. Since that time it is known that materials and structures showing the negative Poisson's ratio do exist in nature. Auxetic materials constitute a new class of materials that not only can be found in nature, i.e., cubic elemental metals, but can also be fabricated, including honeycombs, polymeric and metallic foams, and microporous polymers [9]. Materials with negative Poisson's ratio show unique and strengthened mechanical properties (indentation resistance, mechanical hardness, toughness, and stiffness, damping and acoustic properties) compared to the conventional materials.

A variety of auxetic geometries have been developed and presented by other authors in previous works [10-14]. A comprehensive updated review of auxetic materials, their types and properties, and applications have been presented by Saxena et al. [13].

Based on the deformation mechanism, the auxetic cellular structures have been classified by authors into three types: a) re-entrant type; b) chiral type; and c) rotating units. These types of structures have been recently investigated by many researchers. In particular, Strek and co-authors [15] presented, among other, sinusoidal ligament structures with small amplitude of sinusoidal geometry (stiff structures) of which was stiff and characterized by negative PR, when the structure is compressed or by positive PR during stretching.

Another examples of auxetic materials are a composite material having no voids within their internal structure and yet exhibiting auxetic behavior: two-phase composites or structures have been presented recently [16-22].

In 2004, Scarpa and co-authors showed that foam with the negative Poisson's shows an overall superiority regarding damping and acoustic properties compared to the original conventional foam [23]. Dynamics of auxetic structures made of positive materials were also investigated by other researchers [24-28].

In this paper, a forced response of plate with viscoelastic auxetic damper located at the free end of the plate is investigated. Damping elements involving layers of viscoelastic material with positive or negative Poisson's ratio. Viscoelastic is often used for reduction of vibration (seismic or wind induced vibrations in building structures or other structures) [29-30]. The common feature is that the frequency of the forced vibrations is low. It is assumed that these frequencies are not greater than 10 Hz. Calculations are made using finite element method with Comsol Multiphysics software.

2. Model and material

2.1. *Governing equations*

The Navier's equation of motion with the linear constitutive relation between stresses and deformations is:

$$\rho\frac{\partial^2\mathbf{u}}{\partial t^2} - \nabla\cdot\mathbf{S} = \mathbf{F}_\mathrm{v} \tag{1}$$

where: ρ is the density**,** $\mathbf{u}$ is the vector of displacements, $\mathbf{S}$ is stress tensor and $\mathbf{F}_\mathrm{v}$ is volume force.

The total stress $\mathbf{S}$ in Hooke's law is then augmented by the viscoelastic stress $\mathbf{S}_\mathrm{q}$ and the external stress $\mathbf{S}_\mathrm{ext}$

$$\mathbf{S} = \mathbf{S}_\mathrm{ad} + \mathbf{C}:\boldsymbol{\varepsilon}_\mathrm{el} \tag{2}$$

$$\mathbf{S}_\mathrm{ad} = \mathbf{S}_0 + \mathbf{S}_\mathrm{ext} + \mathbf{S}_\mathrm{q} \tag{3}$$

While elastic strain tensor $\boldsymbol{\varepsilon}_\mathrm{el}$ represents the total strain minus initial and inelastic strains

$$\boldsymbol{\varepsilon}_\mathrm{el} = \boldsymbol{\varepsilon} - \boldsymbol{\varepsilon}_0 \tag{4}$$

$$\boldsymbol{\varepsilon} = \frac{1}{2}((\nabla\mathbf{u})^T + \nabla\mathbf{u}). \tag{5}$$

The elastic strain tensor can, in the same way, be decomposed into volumetric and deviatoric components: $\boldsymbol{\varepsilon}_\mathrm{el} = \frac{1}{3}\boldsymbol{\varepsilon}_\mathrm{vol}\mathbf{I} + \boldsymbol{\varepsilon}_\mathrm{dev}$**,** with the volumetric elastic strain given by $\boldsymbol{\varepsilon}_\mathrm{vol} = trace(\boldsymbol{\varepsilon}_\mathrm{el})$ and the deviatoric contribution by $\boldsymbol{\varepsilon}_\mathrm{dev} = dev(\boldsymbol{\varepsilon}_\mathrm{el})$**.**

The Navier's equation of motion with the linear constitutive relation between stresses and deformations is:

$$\rho \frac{\partial^2 \mathbf{u}}{\partial t^2} - (\mu \nabla^2 \mathbf{u} + (\lambda + \mu)\nabla\nabla \cdot \mathbf{u}) = \mathbf{0}. \tag{6}$$

A harmonic displacement is defined by an equation as below:

$$\frac{\partial^2 \mathbf{u}}{\partial t^2} = -\omega^2 \mathbf{u} \tag{7}$$

where: ω is forcing frequency. The displacement vector has the complex form and is defined as:

$$\mathbf{u}(\mathbf{x}) = \mathbf{u}_1(\mathbf{x}) + j\mathbf{u}_2(\mathbf{x}) \tag{8}$$

and the harmonic displacement is a real part of the complex form:

$$\mathbf{u}(\mathbf{x}, t) = Re[\mathbf{u}(\mathbf{x})\mathrm{e}^{-j\omega t}] \tag{9}$$

According to aforementioned equations the harmonic equation of motion of linear elastic material fulfills a formula:

$$-\rho\omega^2 \mathbf{u} - (\mu \nabla^2 \mathbf{u} + (\lambda + \mu)\nabla\nabla \cdot \mathbf{u}) = \mathbf{0} \tag{10}$$

where: μ, λ are Lamé constants. The harmonic equation may be viewed as the eigenvalue equation.

In the case of viscoelastic material the harmonic equation of motion fulfills the formula:

$$\rho\omega^2 \mathbf{u} - \nabla \cdot \mathbf{S} = \mathbf{F}\mathrm{e}^{i\phi}. \tag{11}$$

$$\mathbf{S} = \mathbf{S}_{\mathrm{ad}} + \mathbf{C}\colon \boldsymbol{\varepsilon}_{\mathrm{el}} - (trace(\mathbf{C}\colon \boldsymbol{\varepsilon}_{\mathrm{el}})/3 + p_w)\mathbf{I} \tag{12}$$

The trace of an n-by-n square matrix **A** is defined as the sum of the elements on the main diagonal (the diagonal from the upper left to the lower right): $trace(\mathbf{A}) = \sum_i A_{ii}$.

2.2. *Model of viscoelastic material*

A convenient way of describing the time-dependent viscoelastic response is to use the spring-dashpot models of material [29-31]. The generalized Maxwell, standard linear solid and Kelvin-Voigt model is the most popular models of viscoelastic materials. All the models are linear, and the corresponding materials can be described as consisting of one or more branches with a spring and a dashpot acting in parallel to a linear elastic material. For each viscoelastic branch, the shear modulus and the relaxation time (or viscosity) are introduced.

The relaxation shear modulus function (or just relaxation function) function $G(t)$ can be found by measuring the stress evolution in time when the material is held at a constant strain. The relaxation function is often approximated by a Prony series:

$$G(t) = G + \sum_{m=1}^{N} G_m exp(-\frac{t}{\tau_m}) \tag{13}$$

A physical interpretation of this approach often called the generalized Maxwell model with G is the stiffness of the main elastic branch, G_m represents the stiffness of the spring in branch m, and τ_m is the relaxation time constant of the spring-dashpot pair in branch m (see Figure 1).

The shear modulus of the elastic branch G is normally called the long-term shear modulus, or steady-state stiffness, and is often denoted with the symbol G_∞. The instantaneous shear modulus G_0 is defined as the sum of the stiffness of all the branches $G(t=0) = G_0 = G + \sum_{m=1}^{N} G_m$. This is the stiffness when the external load is applied much faster than the shortest relaxation time of any viscous branch.

Consequently, we can write the relaxation function (13) as:

$$G(t) = G_0 - \sum_{m=1}^{N} G_m + \sum_{m=1}^{N} G_m \, exp\left(-\frac{t}{\tau_m}\right) = G_0 - \sum_{m=1}^{N} G_m \left(1 - exp(-\frac{t}{\tau_m})\right). \quad (14)$$

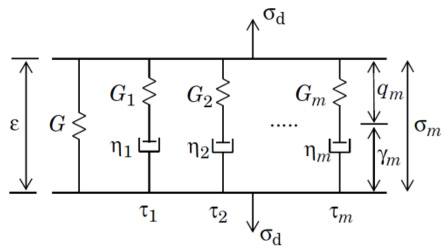

Figure 1. Generalized Maxwell model with m branches (a spring-dashpot pair)

The relaxations time τ_m is normally measured in the frequency domain, so the viscosity of the dashpot is not a physical quantity but instead, it is derived from stiffness and relaxation time measurements. The viscosity of each branch can be expressed in terms of the shear modulus and relaxation time as $\eta_m = G_m \tau_m$. The sum of the stresses in the viscoelastic branches as: $\mathbf{S}_q = \sum_{m=1}^{N} G_m \, q_m = \sum_{m=1}^{N} G_m \, (\varepsilon - \gamma_m)$, where q_m is the auxiliary strain variable introduced to represent the extension of the corresponding abstract spring.

Using Fourier transforms the time-dependent shear relaxation modulus can be expressed in the frequency domain as

$$G = G_s + jG_l \quad (15)$$

where G_s is storage modulus and G_l is loss modulus defined as Prony's series

$$G_s = \sum_m G_m \frac{(\omega\tau_m)^2}{1+(\omega\tau_m)^2} \quad (16)$$

$$G_l = \sum_m G_m \frac{\omega\tau_m}{1+(\omega\tau_m)^2} \quad (17)$$

$$\mathbf{S}_q = 2(G_s + jG_l) \, dev(\boldsymbol{\varepsilon}_{el}) \quad (18)$$

where $dev(\boldsymbol{\varepsilon}_{el})$ is the deviatoric of strain tensor.

3. Numerical results

The viscoelastic layers of dampers mounted on the steel plate are modeled by the generalized Maxwell model. The generalized Maxwell model represents the viscoelastic material as a series of branches, each with a spring-dashpot pair. Eighteen viscoelastic branches guarantee accurate representation of the material behavior for a wide range of excitation frequencies when the damper is subjected to forced vibration. The values of the shear moduli and relaxation times for each branch used in this research were presented by Park [30] and are summarized in Table 1. Material parameters (Young's modulus, Poisson's ratio, bulk modulus, $K = E/(3 \cdot (1 - 2\nu))$, and shear modulus, $G = E/(2 \cdot (1 + \nu))$, of the plate and viscoelastic dampers are presented in Table 2. The steel plate is fixed on the left boundary and free on the right boundary. Damper on the right side of the plate is harmoniously loaded at the top boundary with a total force amplitude $\mathbf{F} = [0, F, 0]$ with $F = 1000$ N. Dampers consists of steel and viscoelastic layers and are mounted on both sides of the plate (see Figure 2). Steel is marked in gray and the viscoelastic material is in blue. The thickness of the plate is 0.004 m, length is 0.2 m and width is 0.1 m. Damper thickness is 0.014 m and thickness of the viscoelastic material is 0.01 m.

Table 1. The values of the shear moduli and relaxation times for 18 branches [30]

Branch, m	Shear modulus, G_m [MPa]	Relaxation time, τ_m [s]	Branch, m	Shear modulus, G_m [MPa]	Relaxation time, τ_m [s]
1	13.3	1e-7	10	4.15	1e-2
2	286	1e-6	11	2.03	3.16e-2
3	291	3.1e-6	12	1.11	1e-1
4	212	1e-5	13	0.491	3.16e-1
5	112	3.16e-5	14	0.326	1
6	61.6	1e-4	15	0.0825	3.16
7	29.8	3.16e-4	16	0.126	10
8	16.1	1e-3	17	0.0373	100
9	7.83	3.16e-3	18	0.0118	1000

Table 2. Parameters of materials of the plate and viscoelastic material

Parameter	Steel AISI 4340	Classic material	Cork material	Auxetic material A	Auxetic material B
Young's modulus, E [Pa]	205e9	2e5	2e5	2e5	2e5
Poisson's ratio, ν [-]	0.28	0.4	0	-0.5	-0.9
Bulk modulus, K [Pa]	1.553e11	3.3333e5	66667	33333	23810
Shear modulus, G [Pa]	8.0078e10	71429	1e5	2e5	1e6
Density, ρ [kg/m^3]	7850	1060	1060	1060	1060

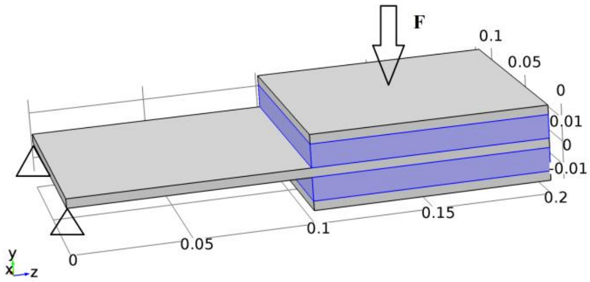

Figure 2. The geometry of plate fixed on the left side and the harmonically loaded on the damper mounted on right side of the plate

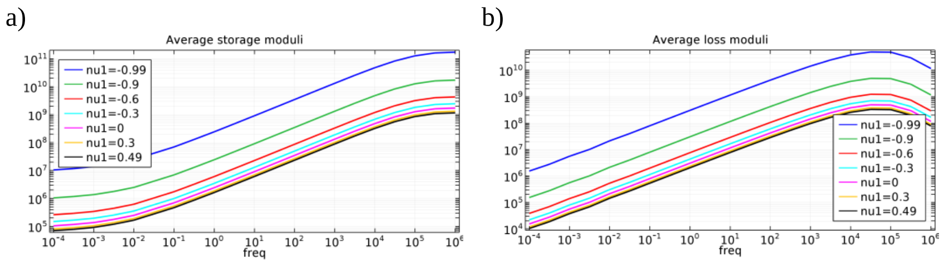

Figure 3. Average value of (a) storage and (b) loss moduli for the viscoelastic material of damper

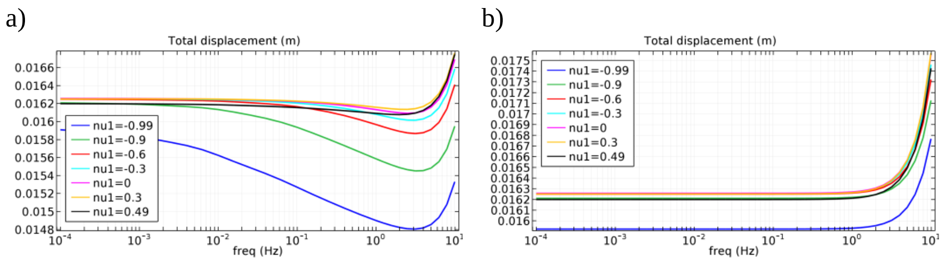

Figure 4. The average amplitude of displacement of the plate for different Poisson's ratio of (a) viscoelastic material and (b) elastic material of damper

Average stores moduli and loss of the viscoelastic material with different Poisson's ratio of dampers mounted on the plate are presented in Figure 3. Both axes are with the logarithmic scale to show changes in the characteristics. Value of both modulus generally increase and depends on a considered range of frequency. Calculations were made for a range of frequency from 10^{-4} to 10^{6} Hz calculated with step $10^{0.25}$ Hz. Value of storage moduli depends on the frequency of motion. The moduli are highest for auxetic viscoelastic material ($\nu = -0.99$) and smallest for classic material with positive Poisson's ratio ($\nu = 0.49$).

In the considered problem, the analysis was made for the plate with mounted dampers with viscoelastic and elastic properties. Comparison of amplitudes of motion of plate is presented in Figure 4. Calculations were made for a range of frequency from 10^{-4} to 10^{1} Hz with step $10^{0.2}$ Hz. Finite element method was used to solve Navier's equation with Comsol Multiphysics software. Second order Lagrange polynomial shape functions and tetrahedral elements were used. The number of mesh elements was 9899 (vertex elements: 28, edge elements: 50, boundary elements: 60) and the number of degrees of freedom was 48522.

The average amplitude of displacement of the right edge of the plate is frequency-dependent and is calculated for the lowest located boundary of the considered geometry. For assumed values of Poisson's ratio of the material of damper, the minimum value of average displacement is for frequency: about 3 Hz in the case of viscoelastic material and close to 0 Hz for an elastic material. The smallest values of total displacement of the plate are achieved for a whole range of considered frequencies for $\nu = -0.99$ for vthe iscoelastic and elastic material of dampers.

4. Conclusions

In this paper, a forced response of a plate with viscoelastic auxetic damper located at the free end of the plate was studied. Damper consists of two layers: steel cover layer and layer of viscoelastic material with positive or negative Poisson's ratio. Viscoelastic materials are often used for reduction of vibration. The common feature is that the frequency of the forced vibrations is low. Calculations were made using finite element method with Comsol Multiphysics software.

Values of stores and loss moduli depend on the frequency of load and motion. The storage moduli are highest for auxetic viscoelastic materials and smallest for classic material with positive Poisson's ratio. The average amplitude of displacement of the plate for different Poisson's ratio of viscoelastic material and elastic material of damper are compared. It was shown that the minimum value of the average displacement is for frequency: about 2 Hz in the case of viscoelastic material and close to 0 Hz for an elastic material.

Acknowledgments

This work was supported by grants of the Ministry of Science and Higher Education in Poland: 02/21/DS-PB/3513/2018. The simulations have been made at the Institute of Applied Mechanics, Poznan University of Technology.

References

1. L. J. Gibson, *The elastic and plastic behaviour of cellular materials*, University of Cambridge, Churchill College (doctoral thesis) 1981.
2. L. J. Gibson, M. F. Ashby, G. S. Schayer, C.I. Robertson, *The mechanics of two-dimensional cellular materials*, Proc. Roy. Soc. Lond. A **382** (1982) 25 – 42.

3. L. J. Gibson, M.F. Ashby, *The mechanics of three-dimensional cellular materials*, Proc. Roy. Soc. Lond. A **382** (1982) 43 – 59.
4. L. J. Gibson, M. F. Ashby, *Cellular Solids: Structure and Properties*, 2nd ed.; Pergamon Press: London, UK, 1988.
5. R. F. Almgren, *An isotropic three-dimensional structure with Poisson's ratio =−1*, Journal of Elasticity **15** (1985) 427 – 430.
6. K. W. Wojciechowski, *Constant thermodynamic tension Monte Carlo studies of elastic properties of a two-dimensional system of hard cyclic hexamers*, Molecular Physics **61** (1987) 1247 – 1258.
7. R. Lakes, *Foam structures with a negative Poisson's ratio*, Science, **235** (1987) 1038 – 1040.
8. R. Lakes, *Advances in negative Poisson's ratio materials*, Advanced Materials (Weinheim), **5**(4) (1993) 293 – 296.
9. X. Zhang, D. Yang, *Mechanical Properties of Auxetic Cellular Material Consisting of Re-Entrant Hexagonal Honeycombs*, Materials (Basel), **9**(11) (2016) 900.
10. Y. Prawoto, *Seeing auxetic materials from the mechanic point of view: A structural review on the negative Poisson's ratio*, Computational Materials Science, **58** (2012) 140 – 153.
11. J. C. A. Elipe, A. D. Lantada, *Comparative study of auxetic geometries by means of computer-aided design and engineering*, Smart Mater. Struct., **21(10)** (2012) 105004.
12. T. C. Lim, *Auxetic Materials and Structures*, Springer-Verlag, Singapur, 2015.
13. K. K. Saxena, R. Das, E. P. Calius, *Three Decades of Auxetics Research Materials with Negative Poisson's Ratio: A Review*, Adv. Eng. Mater., **18** (2016) 1847 – 1870.
14. H. M. A. Kolken, A. A. Zadpoor, *Auxetic mechanical metamaterials*, RSC Adv., **7**, (2017) 5111.
15. T. Strek, H. Jopek, K. W. Wojciechowski, *The influence of large deformations on mechanical properties of sinusoidal ligament structures*, Smart Mater. Struct., **25** (2016) 054002 (10pp).
16. D. Li, J. Maa, L. Dong, R. S. Lakes, *A bi-material structure with Poisson's ratio tunable from positive to negative via temperature control*, Materials Letters, **181** (2016) 285 – 288.
17. T. Strek, H. Jopek, E. Idczak, K. W. Wojciechowski, *Computational Modelling of Structures with Non-Intuitive Behaviour*, Materials, **10** (2017) 1386.
18. T. Strek, A. Matuszewska, H. Jopek, *Finite element analysis of the influence of the covering auxetic layer of plate on the contact pressure*, Phys. Status Solidi B, **254(12)** (2017) 1700103.
19. H. Jopek, *Finite Element Analysis of Tunable Composite Tubes Reinforced with Auxetic Structures*, Materials, **10** (2017) 1359.
20. H. Jopek, T. Strek, *Torsion of a two-phased composite bar with helical distribution of constituents*, Phys. Status Solidi B, **254**(12) (2017) 1700050.
21. E. Idczak, T. Strek, *Minimization of Poisson's ratio in anti-tetra-chiral two-phase structure*, IOP Conf. Series: Materials Science and Engineering **248** (2017) 012006.

22. E. Idczak, T. Strek, *Dynamic Analysis of Optimized Two-Phase Auxetic Structure*, Vibrations in Physical Systems, **28** (2017) 2017003-01-20017003-12.
23. F. Scarpa, L. G. Ciffo, J. R. Yates, Dynamic properties of high structural integrity auxetic open cell foam, Smart Mater. Struct., **13** (2004) 49.
24. R. Lakes, T. Lee, A. Bersie, Y. C. Wang, Extreme damping in composite materials with negative-stiffness inclusions. Nature, **410** (2001) 565 – 567.
25. M. Nienartowicz, T. Stręk, Finite Element Analysis of Dynamic Properties of Thermally Optimal Two-Phase Composite Structure, Vibrations in Physical Systems, **26** (2014) 203 – 210.
26. T. Strek, H. Jopek, M. Nienartowicz, Dynamic response of sandwich panels with auxetic cores, Phys. Status Solidi B**, 252**(7) (2015) 1540 – 1550.
27. E. Idczak, T. Stręk, Computational Modelling of Vibrations Transmission Loss of Auxetic Lattice Structure, Vibrations in Physical Systems, **27** (2016) 124 – 128.
28. W. Liu, M. Wang, T. Luo, Z. Lin, In-plane dynamic crushing of re-entrant auxetic cellular structure, Materials & Design, **100** (2016) 84 – 91.
29. K. L. Shen, T. T. Soong, *Modeling of Viscoelastic Dampers for Structural Applications*, J. Eng. Mech., **121** (1995) 694 – 701.
30. S. W. Park, *Analytical Modeling of Viscoelastic Dampers for Structural and Vibration Control*, Int. J. Solids and Structures, **38** (2001) 8065 – 8092.
31. D. Gutierrez-Lemini, *Engineering Viscoelasticity*, Springer, New York 2014.